



# Modeling, Kinetic and Experimental optimization of Reforming Unit for Al- Doura Heavy Naphtha over bi and Tri-metallic Catalysts

Ramzy S. Hamied<sup>1,\*</sup>, Khalid A. Sukkar<sup>2</sup>, Shahrazad R. Raouf<sup>2</sup>

<sup>1</sup>Petroleum Technology Department, University of Technology– Iraq.

<sup>2</sup>Chemical Engineering Department. University of Technology– Iraq.

## Article information

### Article history:

Received: January, 19, 2022

Accepted: February, 25, 2022

Available online: April, 8, 2022

### Keywords:

Catalytic Reforming

Tri-metal catalysts

Heavy Naphtha

### \*Corresponding Author:

Full Name: Ramzy S. Hamied

[150002@uotechnology.edu.iq](mailto:150002@uotechnology.edu.iq)

## Abstract

In the present work, experimental and mathematical model were simulated to describe the catalytic reforming process reaction, using Iraqi heavy naphtha as a feed stock. Tri and bi-metal catalysts were prepared by adding the tin and iridium (Ir) to the classical catalyst used in catalytic reforming unit in Al – Doura refinery to enhance the reaction selectivity. The effect of the main three catalytic reforming reactions, named dehydrogenation, hydrocracking, and dehydrocyclization, on the catalyst performance (activity and selectivity) were investigated. Catalysts performances were investigated under the following operating condition: constant reaction pressure equal to 6 atm, the reaction temperature range of (480, 490, 500, and 510 °C), constant hydrogen to hydrocarbon ratio of 4:1, and WHSV (weight hour space velocity) range of (1, 1.5, and 2 hr<sup>-1</sup>).

The results show that as reaction temperature increase, higher conversion of Paraffins and Naphthenes components in Iraqi heavy naphtha while negative impact on conversion as weight hourly space velocity increases (i.e., higher WHSV shows lower conversion). Generally, tri and bi-metal catalysts the aromatics and light components yields will be increased under the same operating conditions reforming process.

Simulation and mathematical representation and was developed to describe the catalytic reforming reactions kinetics. Mathematical model predicts the conversion, temperature and concentration profile with time and axial direction are considered. Simulation and progressing model agreement with the results of experimental work according to the suggested scheme for heavy naphtha catalytic reforming of network reactions, the deviation results when comparison of experimental and mathematical model results equal to 19.5%.

DOI: <http://doi.org/10.55699/ijogr.2022.0201.1020>, Department of Petroleum Technology, University of Technology-iraq

This is an open access article under the CC BY 4.0 license <http://creativecommons.org/licenses/by/4.0>

## 1. Introduction

Petroleum refineries consist of several thermal and catalytic units used to convert and separate petroleum fractions into useful products. Naphtha reforming units convert low-octane number heavy naphtha into a higher-octane number reformate that is the main feedstock for the blending unit to produce gasoline [1, 2].

The catalytic reforming process of naphtha has been developed rapidly over the past four decades and has become one of the most advanced units in the refining industry. The various reforming reactions are dehydrogenation reactions of the paraffins to naphthenes and dehydrogenation of the naphthenes to aromatics, dehydrocyclization of paraffins to naphthenes, isomerization of normal paraffins to iso-paraffins, cracking of paraffins and naphthenes and hydrodealkylation of aromatics. Modelling and simulation of catalytic reforming has been considered by many researchers to determine the plant performance or product distribution behavior [3, and 4].

The metals used with Pt/ Al<sub>2</sub>O<sub>3</sub> catalyst are Sn, Ir, and Ge. These additives modify their activity, selectivity, stability of the catalyst, and lower coking rate and their higher resistance to deactivation. These metals are used as bi- and tri-metallic catalysts. This type of bi- and tri-metallic naphtha reforming catalyst makes a big leap forward in the technology of reforming catalyst and it improves its properties of this catalysts. [5 and 6].

Askari 2012 developed model for simulating catalytic reforming unit with four reactors in series by using Hysys-refinery software. The results were validated by operating data, taken from the Esfahan oil refinery catalytic reforming unit [7]. Elizalde and Ancheyta 2015 proposed the dynamic modeling of the catalytic naphtha reforming reactor using material and heat balances; the reaction network consisted of 20 components plus hydrogen and 53 chemical reactions [8]. Dong et al. 2018 described a continuous catalytic reforming process using a kinetic model of 27-lump, plug flow reactor model of a 4-zone parallel-series and an empirical catalyst deactivation model. The mean absolute prediction was found to be 0.76%, 0.42%, 0.90%, and 0.50% for PNAH, respectively [9]. Xiao yang Yi et al. 2020 constructed kinetic model for the naphtha reforming process. By assembling the components into reactivity based lumps, a new reaction network model rooted on 33 lumps and 101 reactions was studied. The search algorithm was used to determine the global optimal solution. By comparing with the test data, the average deviation of the reformed products calculated from the proposed model reached 2.5% [10].

The objective of this work is to develop classical catalysts used in reforming units by preparation bi- and tri-metallic catalysts and study the performance of these catalysts under different operating conditions using Al-Dura heavy naphtha a feed stock. Also, the mathematical representation was used to describe the reactions of catalytic reforming, kinetics parameters (pre-exponential factors, activation energy, heat of reactions optimum operating conditions) for prepared catalysts.

## 2. Experimental

### 2.1. Materials

The properties of Al-Dura heavy naphtha are shown in Table (1). Nitrogen was purchased from the Dijlah factory, analyzed by GC and confirms its purity of 99.9%. In order to reduce oxygen and water impurities a molecular sieve type (5A) which has been installed on the line of hydrogen.

**Table (1): Al-Dura heavy naphtha properties.**

Property	Unit	Data	Property	Unit	Data	
Specific Gravity at 15.6 °C	-	0.733	Total distillate	vol%	98.5	
API	-	61.7	Total recovery	vol%	99.5	
Distillation			Residue	vol%	1	
	I.B.P	°C	60	Loss	vol%	0.5
	10 vol % distilled	°C	88	Sulfur Content	ppm	3
	50 vol % distilled	°C	117	Mwt.	g/gmol	108
	90 vol % distilled	°C	147	Total Paraffin	vol %	60
F.B.P	°C	178	Total naphthene & aromatic	vol %	40	

### 2.1. Catalysts

The catalysts used in reforming units (Al-Dura refinery) were Pt /  $\gamma$ -Al<sub>2</sub>O<sub>3</sub> (RG 412), and Pt-Re /  $\gamma$ -Al<sub>2</sub>O<sub>3</sub> (RG 482) catalysts. The prepared catalysts in the lab (Pt-Ir /  $\gamma$ -Al<sub>2</sub>O<sub>3</sub> and Pt-Re- Sn /  $\gamma$ -Al<sub>2</sub>O<sub>3</sub>). The

properties (physical and chemical) for the catalysts were measured in Oil Research and Development Center / Ministry of Oil, as shown in Table (2):

**Table (2): Properties of commercial and prepared catalysts.**

	Commercial Pt/ $\gamma$ -Al <sub>2</sub> O <sub>3</sub>	Commercial Pt-Re/ $\gamma$ -Al <sub>2</sub> O <sub>3</sub>	Prepared Pt-Ir/ $\gamma$ -Al <sub>2</sub> O <sub>3</sub>	Prepared Pt-Re-Sn/ $\gamma$ -Al <sub>2</sub> O <sub>3</sub>
Pt, wt %	0.35	0.3	0.5	0.3
Re, wt %	-	0.3	-	0.3
Sn, wt %	-	-	-	0.1
Ir, wt %	-	-	0.1	-
Form	Extrudate	Extrudate	Extrudate	Extrudate
Surface Area (m <sup>2</sup> /g)	220	220	219.9	196
Pore Volume (cm <sup>3</sup> /g)	0.57	0.6	0.61	0.73
Bulk Density (g/cm <sup>3</sup> )	0.66	0.69	0.67	0.685

#### 2.2.1.1. Preparation of Platinum- Rhenium -Tin / Alumina Catalyst

The catalyst was prepared by co-impregnation by adding tin chloride (SnCl<sub>2</sub>.2H<sub>2</sub>O) to platinum- rhenium supported on alumina catalyst in order to reach a final concentration of 0.3 wt% Pt, 0.3 wt% Re and 0.1 wt% Sn [1]. SnCl<sub>2</sub> was first dissolved in deionized water and heated for 30 min at 70 °c. Tin chloride was added to the solution containing catalyst and left without stirring for 1 hr and then gently stirred for (1/2-1 hr) in the water bath at 70 °C. Then, the catalyst was dried at 120 °C for 12 hrs, and calcined in air at 500 °C for 4 hrs and finally reduced in hydrogen at 500 °C for 4 hrs at hydrogen flow of 80 cm<sup>3</sup>/min.

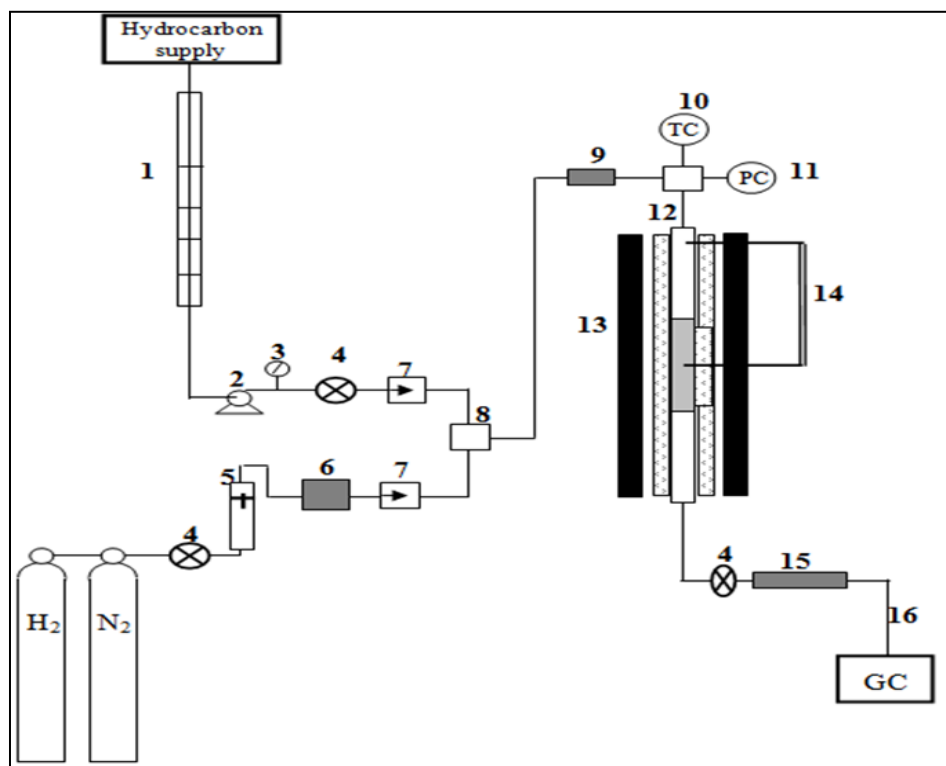
#### 2.2.2. Preparation of Platinum-Iridium / Alumina Catalyst

The catalyst was prepared by impregnation the parent catalyst (Pt/Al<sub>2</sub>O<sub>3</sub>) with Iridium chloride (IrCl<sub>3</sub>) in order to reach final concentration of 0.5 wt% of Pt and 0.1 wt% of Ir [10]. Iridium chloride was added to the slurry solution of HCl and support and gently stirred for 1 hr at room temperature. The slurry was left into water bath at 70 °C. Then dried at 120 °C overnight. The catalysts were finally calcined in air at 300 °C for 4 hrs and then reduced by flowing hydrogen at (60 cm<sup>3</sup>/min) at 500 °C for 4 hrs. Heating ramps were programmed every 10 °C /min.

#### 2.2.3. Heavy Naphtha Catalytic Reforming Unit and Operating Procedure

The heavy naphtha catalytic activities are carried out in a conventional continuous flow vertical tubular reactor, the reactor dimensions are 20mm internal diameter, 30mm external diameter and 68cm height (reactor volume 214 cm<sup>3</sup>). The reactor was charged with 50g (the bed catalyst is 22 cm) of catalyst located in the middle zone for each experiment, the reactor upper and lower zones filled with glass beads. The products were cooled and collected in a separator in order to exhaust the gases to the atmosphere and collect the condensed liquid from bottom of the separator. Product samples were analyzed using gas chromatography (Shimadzu 2014 GC). Figure (1) shows the pilot plant of catalytic reforming unit.

The catalytic reforming reaction was tested at temperatures (480, 490, 500, and 510 °C), the pressure was kept constant at 6 atm. Heavy naphtha weight hourly space velocities were varied at (1, 1.5, and 2 hr<sup>-1</sup>), hydrogen to hydrocarbon molar ratio kept constant at 4:1. The reactivation carried at 450 and 500 °C for four hours respectively in a current of hydrogen at atmospheric pressure and flow ratio (60 and 80 cm<sup>3</sup>/min). Heavy naphtha pumped under pressure to the reforming unit. The deactivation catalyst was ignored because the fresh catalyst was used for each run.



1-Metering burette	9- Feed preheating zone
2-Dosing pump	10 - Temperature controller system
3-Liquid flow meter	11- Pressure controller system
4-Needle valve	12- Stainless steel reactor
5- H <sub>2</sub> flow meter	13- Heating furnace
6- 5A – Molecular sieve dryer	14- Thermocouples system
7- One way valve	15- Cooling system
8- Mixing section	16- Gas chromatography

Figure (1): Pilot plant of catalytic reforming unit

## 4. Simulation and Mathematical Model

### 4.1. Description of mathematical model and Assumptions

The main object of the present study is to analyze the catalytic reforming process kinetics by evaluating the different effects of reaction temperature and reaction time and on the substrate contained in the course of the process by using Iraqi heavy naphtha as feedstock. In this work three groups of compounds were found: normal and iso paraffins (P), naphthenes (N), and aromatics (A). Catalytic reforming process model with mass and energy balances, kinetic thermodynamic, concentration, and temperature distributions along the length reactor can be estimated.

Progressing the reactor model of catalytic reforming process assumptions is shown below:

- Isothermal operation plugs flow and steady state process.
- Effect of the pressure constant throughout operation.
- The limiting step was the surface reaction.
- Reactant and products density are constant.
- The temperature and concentration gradients along axial direction are considered and the radial direction can be neglected.
- Constant catalyst activity for calculation, all the rate equations are linear pseudo-monomolecular in nature, and all the reforming reactions rates are first order (proved experimentally).

4.2. Reaction Kinetics

Catalytic reforming of Iraqi heavy naphtha for the present work, monitoring and analysis of the consecutive and parallel heterogeneous reaction, the network reactions suggest are schematically represented in Figure (2).

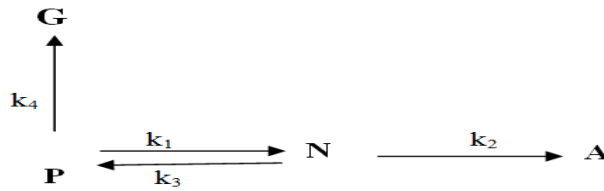


Figure (2) heavy naphtha catalytic reforming reactions network.



The simple power law kinetic expression for reactions (1,2, and 3) is considered [11]:

$$r_1 = k_1 C_P - k_3 C_N P_{H_2} \dots(4), \quad r_2 = k_2 C_N \dots\dots\dots(5), \quad r_3 = k_4 C_P \dots\dots\dots(6)$$

Reaction Rate general form is:  $r_i = k_i C_i^n$  .....(7)

where,  $k_i = A_o EXP\left(\frac{-E_a}{RT}\right)$  .....(8)

The Arrhenius expression confirms the reaction rate constant k<sub>i</sub> [11]:

$$Ln k_i = Ln A_o - \frac{E_a}{RT} \dots\dots\dots(9)$$

The reaction equilibrium constants  $K_{eq} = k_1/k_3$  The following thermodynamic relation, equilibrium constant can be calculated by the [9]  $K_{eq} = EXP\left(\frac{-\Delta G}{RT}\right)$  .....(10)

Under the present reactions first order with respect to reactants therefore the kinetic expression is to be linear.

4.3 Model Kinetic Reaction

4.3.1. Mass Balance

A material balance is made over the cross section of a very short segment of the tubular catalyst bed to develop a reaction model for an integral reactor, as shown in Figure (3):

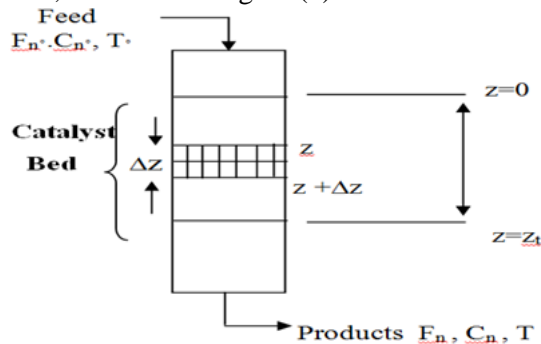


Figure (3) Tubular reactor Segment

Then, the resulting equation [12] is  $F_N|_z - F_N|_{z+\Delta z} - V_{pp}(1-\epsilon)(-r_1) = 0$  .....(11)

As  $\Delta z \rightarrow 0$ , material balance differential reduced to:  $\frac{dF_n}{dV} = -r_i$  .....(12)

Since:  $dw = dv \rho(1-\epsilon)$  ..... (13)

Each component in heavy naphtha feed stocks reaction rate equations can now be developed for Paraffins, Naphthenes and Aromatics: a space time variable,  $\theta$ , as:  $\theta = w/f$  .....(14)

For a constant feed rate, an incremental section of catalyst bed, may expressed as:  $dw = f.d\theta$  .....(15)

4.3.2. Energy Balance

Energy balance over the differential reactor control volume used to estimate the temperature profile along the reactor which is obtained from an [13].

$f \cdot \rho \cdot C_p dT = r_{P \leftrightarrow N} \Delta H_{r,P \leftrightarrow N} dw + r_{N \leftrightarrow A} \Delta H_{r,N \leftrightarrow A} dw + r_{P \rightarrow G} \Delta H_{r,P \rightarrow G} dw$  .....(16)

Equation (15) substituting in to equation (16) obtain:-  $\frac{dT}{d\theta} = \frac{1}{\rho C_p} \left( \begin{matrix} r_{P \leftrightarrow N} \Delta H_{r,P \leftrightarrow N} \\ + r_{N \rightarrow A} \Delta H_{r,N \rightarrow A} \\ + r_{P \rightarrow G} \Delta H_{P \rightarrow G} \end{matrix} \right)$  .....(17)

The above differential equation is taken to be as first order and this is improved experimentally as:-

$-r_i = k_i C_i^n$  ..... (7)

Taking natural logarithm for both side of equation (7) obtain:  $\ln(-r_i) = \ln k_i + n \ln C_i$  .....(18)

Plot  $\ln(-r_i)$  vs.  $\ln C_i$ , the first order behaviors must be straight line, Figures (4) and (5) illustrate that different reaction and different catalyst, for some selected types of both catalysts these two figures are just samples.

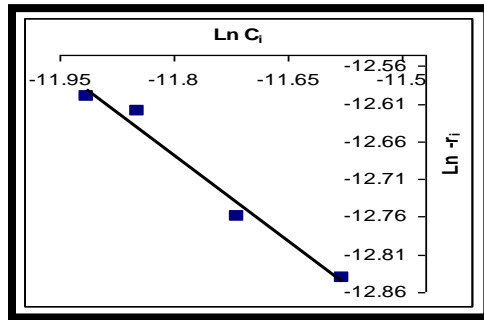


Figure (4) Naphthene +Hydrogen→Paraffin for bi-metal catalyst at 1.5 hr<sup>-1</sup>

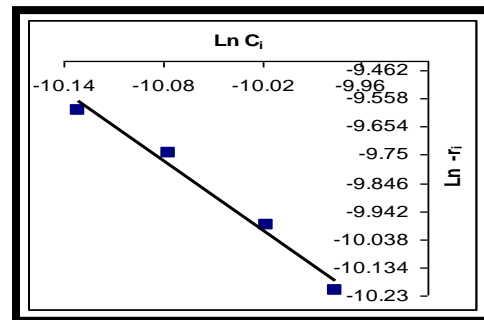


Figure (5) Paraffin →Naphthene +Hydrogen for tri-metal catalyst at 1hr<sup>-1</sup>

4.4. Model Process

Figure (3) show the axial flow reactor model for catalytic reforming process. All the differential equation in the mathematical model numerically solved by method of finite difference approach with explicit solution.

For Mass balance [14]:  $\frac{dY_i}{dZ} = \sum_{i=1}^m \frac{MW}{z \cdot WHSV} (-r_i)$  .....(19)

Iraqi heavy naphtha components (P, N, and A) substitute's in above equation.

$$\text{For energy balance: } \frac{dT}{dZ} = S \frac{\sum_{i=1}^m r_i (-\Delta H_{r_i})}{\sum_{i=1}^m f_i C_{P_i}} \quad \dots\dots\dots(20)$$

$$\frac{dT}{dZ} = \frac{S}{\sum_{i=1}^m f_i C_{P_i}} \left[ \begin{array}{l} r_{P \rightarrow N} (-\Delta H_{r, P \rightarrow N}) \\ + r_{N \rightarrow A} (-\Delta H_{r, N \rightarrow A}) \\ + r_{N \rightarrow P} (-\Delta H_{r, N \rightarrow P}) \\ + r_{P \rightarrow G} (-\Delta H_{P \rightarrow G}) \end{array} \right] \quad \dots\dots\dots(21)$$

$$\Delta H^\circ_{r,T} = \Delta H^\circ_{r,298} + \int_{298}^T \Delta C_p dT \quad \dots\dots\dots(22)$$

Table (3) shows that the results of estimations heat reactions.

**Table (3): Heat of reaction results**

$\Delta H^\circ_r$ (J/mole $H_2$ )				
Reaction	480 °C	490 °C	500 °C	510 °C
$N + H_2 \rightarrow P$	-54393.3	-54238.5	-53903.7	-53648.5
$N \rightarrow A + 3H_2$	73119.9	73207.8	73291.5	73361.2
$P + (n-3/3) H_2 \rightarrow n/15(C_1-C_5)$	-52623.1	-52837.6	-53079.3	-53309.7

#### 4.5. Reaction Kinetic Parameters Estimation

Arrhenius equation were used to estimate the apparent activation energy ( $E_a$ ) which satisfies the relationships between reaction temperature and rate constant as specified in equations (7, 8, and 9). Plot  $\ln(k)$  vs.  $(1/T)$ . Activation energy was calculated from the slope represented by  $(-E_a/R)$  and the intercept represented by  $\ln(A_0)$ . Table (4) list the results of tri and bi- metal catalysts.

**Table (4): Tri and bi-metal catalysts Activation energy and pre-exponential factor**

Reaction	$E_a/R$	$E_a$ (kcal/mol)	$A_0$
<b>Pt-Ir/<math>\gamma</math>-<math>Al_2O_3</math></b>			
$P \rightarrow N + H_2$	15084	29.97	$7.927 \cdot 10^8$
$N + H_2 \rightarrow P$	10674	21.21	$6.733 \cdot 10^5$
$N \rightarrow A + 3H_2$	9822.2	19.52	$7.997 \cdot 10^5$
$P + H_2 \rightarrow 2G$	11905	23.65	$5.803 \cdot 10^6$
<b>Pt-Re-Sn/<math>\gamma</math>-<math>Al_2O_3</math></b>			
$P \rightarrow N + H_2$	17764	35.29	$2.347 \cdot 10^{10}$
$N + H_2 \rightarrow P$	13367	26.56	$2.023 \cdot 10^7$
$N \rightarrow A + 3H_2$	7983.6	15.863	$1.581 \cdot 10^5$
$P + H_2 \rightarrow 2G$	13684	27.19	$5.424 \cdot 10^7$

## 5. Results and Discussion

### 5.1. Temperature Effect

Reaction temperatures influence range between (480 - 510 °C). The wight hour space velocity was ( $1hr^{-1}$ ) for both tri and bi-metal catalyst. From Figures (6 - 13) can be seen that with the increase in the reaction temperature



the concentrations of light components (n-pentane and n-hexane) increased and the concentration % of heavier components decreases as increase of reaction temperatures. This result was attributed to the dehydrocyclization reaction which is preferred at higher reaction temperature and higher molecular weight of carbon number [16]. Increasing temperature and carbon number make the naphthenes dehydrogenation and paraffin's dehydrocyclization became faster. This led to increasing the mole % of aromatics components [17]. The comparison of the results performance between the two prepared tri and bi-metal catalysts shows that tri-metal catalyst had better results than the bi-metal catalyst because the addition of tin to the classical catalyst used in catalytic reforming unit in Al –Doura refinery has enhanced the isomerization reaction selectivity, and also the aromatization reaction increased according to Bednarova et al. [18].

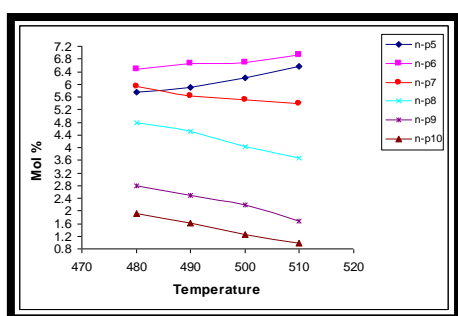


Figure (6) Temperature effect of on the mole % of n-P at 1 hr<sup>-1</sup> whsv for tri-metal catalyst

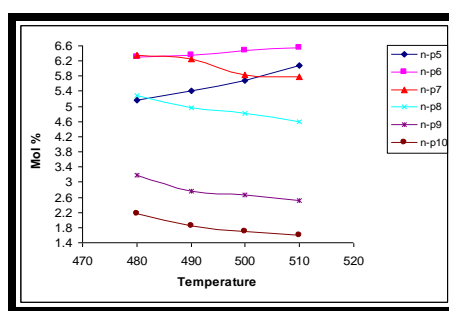


Figure (7) Temperature effect of on the mole % of n-P at 1 hr<sup>-1</sup> whsv for bi-metal catalyst

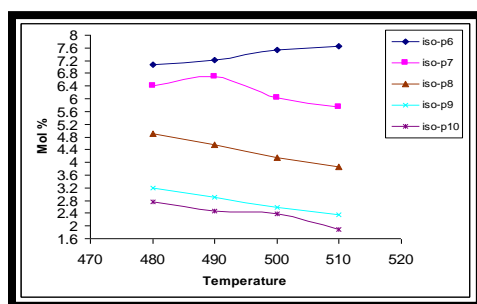


Figure (8) Temperature effect of on the mole % of iso-P at 1 hr<sup>-1</sup> whsv of for tri-metal catalyst

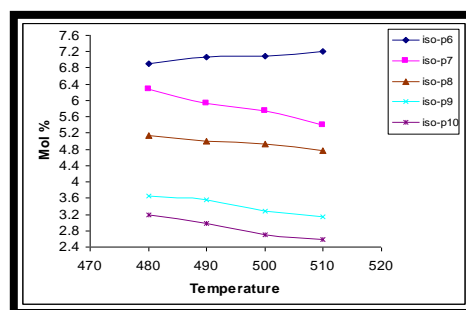


Figure (9) Temperature effect of on the mole % of iso-P at 1 hr<sup>-1</sup> whsv for bi-metal catalyst

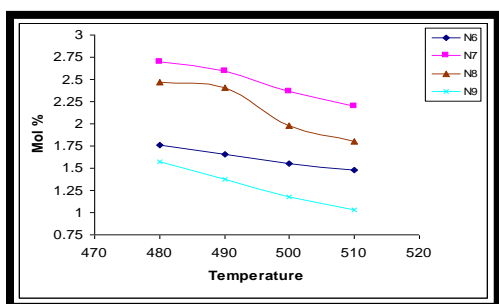


Figure (10) Temperature effect of on the mole % of Naphthene at 1 hr<sup>-1</sup> whsv of for tri-metal catalyst

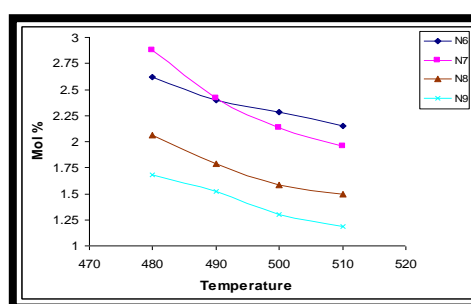


Figure (11) Temperature effect of on the mole % of Naphthene at 1 hr<sup>-1</sup> whsv for bi-metal catalyst



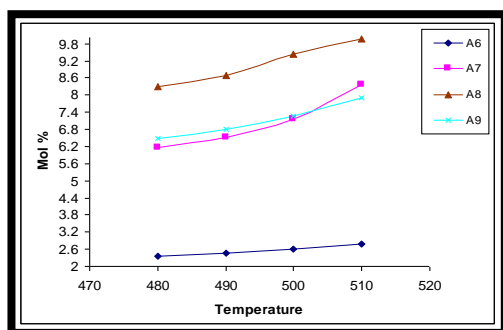


Figure (12) Temperature effect of on the mole % of Aromatics at 1 hr<sup>-1</sup> whsv of for tri-metal catalyst

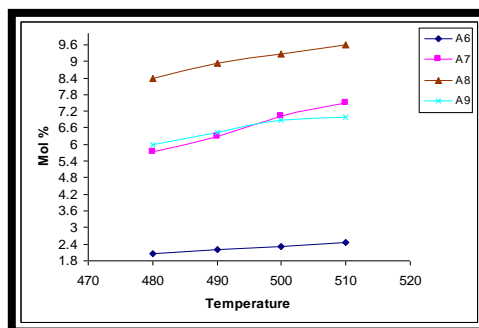


Figure (13) Temperature effect of on the mole % of Aromatics at 1 hr<sup>-1</sup> whsv for bi-metal catalyst

### 5.2. Weight Hour Space Velocity (WHSV) Effect

Weight hour space velocity (WHSV) influence of was studied at ranging between (1, 1.5, and 2 hr<sup>-1</sup>), taking the temperature constant of 510 °C which is the best result of highest aromatics yield. Figures (14- 21) show that as the weight hour space velocity increases mole% of light components n-pentane and n-hexane decreases; the reason for this behavior is hydrocracking reaction became slow rate. Residence time decrease with increase in WHSV, which causes feedstock with the catalyst inside reactor offers plenty of contact time, this will lead to an effective n-paraffins conversion [19]. Weight hour space velocity increases reactivity decreases was observe for the heavier paraffins. This lead to that dehydrocyclization reaction of normal and iso - paraffins is the slowest reaction, therefore aromatics yield decrease.

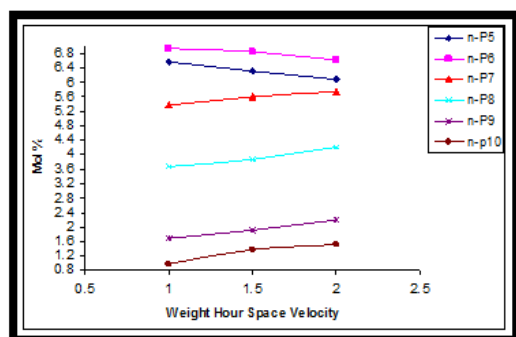


Figure (14) WHSV Effect on the mole % of n-P at 510 °C for tri-metal catalyst

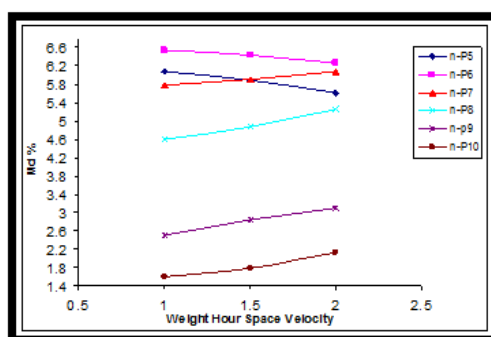


Figure (15) WHSV Effect on the mole % of n-P at 510 °C for bi-metal catalyst

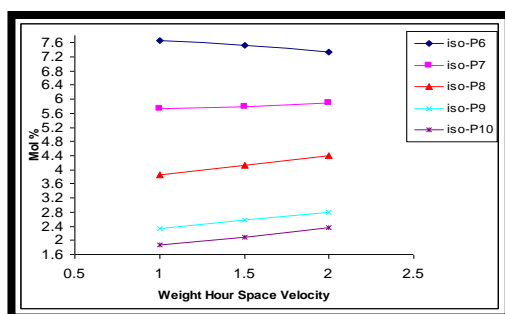


Figure (16) WHSV Effect on the mole % of iso-P at 510 °C for tri-metal catalyst

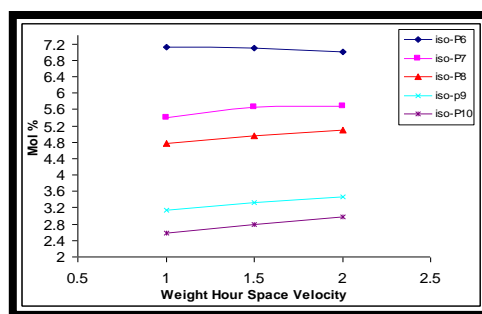


Figure (17) WHSV Effect on the mole % of iso-P at 510 °C for bi-metal catalysts

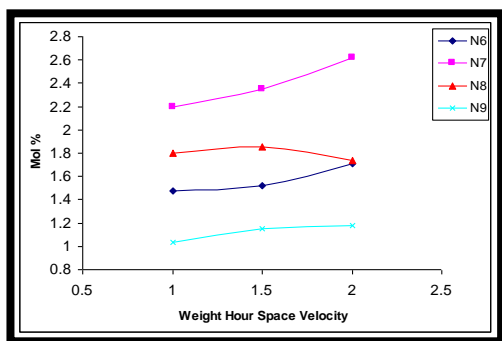


Figure (18) WHSV Effect on the mole % of Naphthenes at 510 °C for tri-metal catalyst

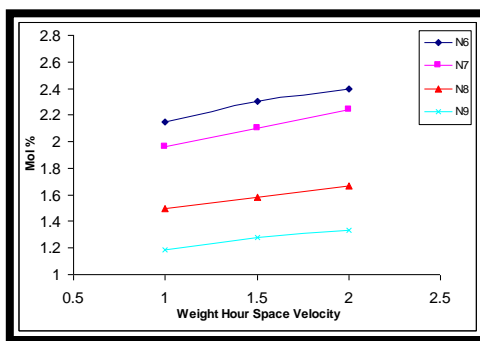


Figure (19) WHSV Effect on the mole % of Naphthenes at 510 °C for bi-metal catalyst

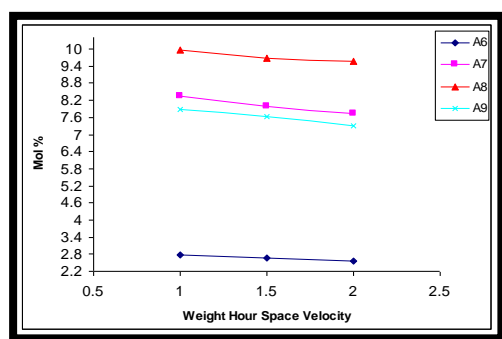


Figure (20) WHSV Effect on the mole % of Aromatics at 510 °C for tri-metal catalyst

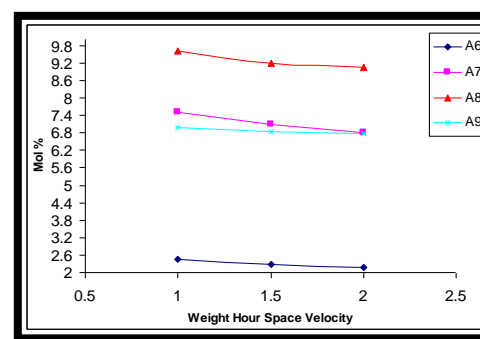


Figure (21) WHSV Effect on the mole % of Aromatics at 510 °C for bi-metal catalyst

### 5.3 Mathematical Model Simulation Results

The concentration profiles of reactants (P and N) and products (A and G) illustrated in figures (22) and (23) for tri and bi-metal catalysts prepared in the present work at temperature (480 °C) and weight hour space velocity of ( $1\text{hr}^{-1}$ ) as an example.

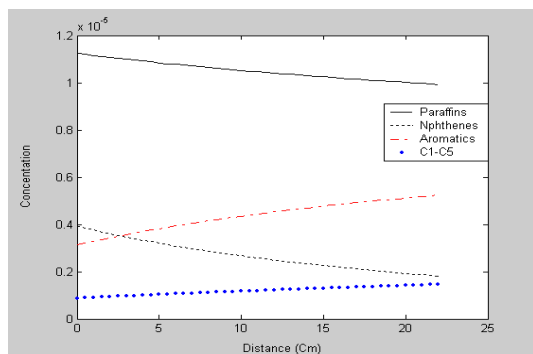


Figure (22) (P, N, A, and G) concentration profiles for tri-metal catalyst

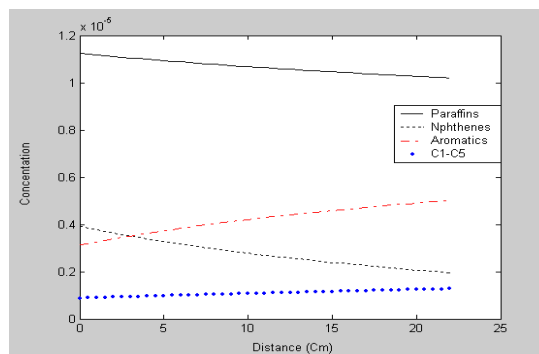


Figure (23) (P, N, A, and G) concentration profiles for bi-metal catalyst

Experimental and predicted comparison for conversion of reactant (P and N) for tri and bi-metal catalysts shown in figures (24) and (25) as example. The comparison between theoretical and experimental results represents in table (5). Results of the experimental work according to the suggested scheme of network reactions

for Iraqi heavy naphtha catalytic reforming agrees with derived model and simulation. Deviation of experimental results compare with the derived model reaches to 19.50%.

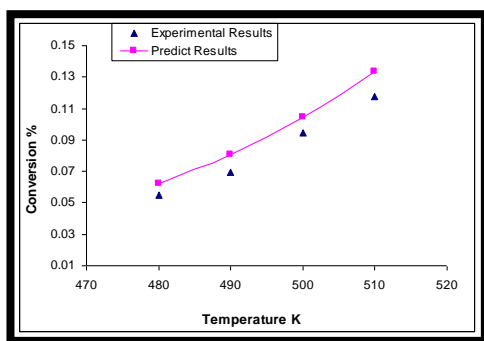


Figure (24) Experimental comparisons with predicted conversion of Paraffins at (1hr<sup>-1</sup>) WHSV for tri-metal catalyst.

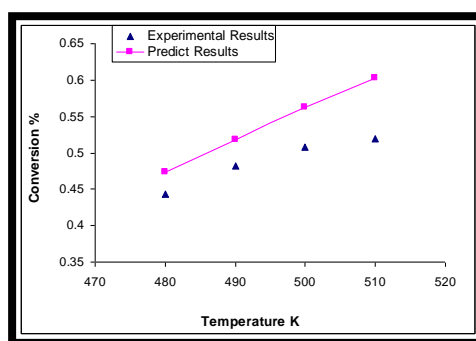


Figure (25) Experimental comparisons with predicted conversion of Paraffins at (1hr<sup>-1</sup>) WHSV for bi-metal catalyst.

Table (5) Experimental and Theoretical mol % for bi-and tri-metal catalyst at 1hr-1 WHSV

Condition	Components	Pt-Re-Sn/ $\gamma$ -Al <sub>2</sub> O <sub>3</sub>		Relative deviation %	Pt-Ir/ $\gamma$ -Al <sub>2</sub> O <sub>3</sub>		Relative deviation %
		Exp. Conv %	Theo. Conv %		Exp. Conv %	Theo. Conv %	
480 °C	Paraffins	5.50	6.21	6.35	48.46	55.49	14.51
490 °C	Paraffins	6.94	8.09	10.07	46.7	46.86	0.36
500 °C	Paraffins	9.44	10.44	3.47	45.25	46.28	2.28
510 °C	Paraffins	11.74	13.32	2.95	44.15	45	1.93
480 °C	Naphthenes	45.60	50.94	9.71	9.24	9.8	6.11
490 °C	Naphthenes	45.57	53.85	15.31	8.13	8.7	7.10
500 °C	Naphthenes	48.07	56.32	13.22	7.29	7.99	9.6
510 °C	Naphthenes	48.10	58.3	19.5	6.8	7.74	13.85
480 °C	Aromatics	1.582	1.779	9.77	22.14	24.59	11.1
490 °C	Aromatics	1.662	1.863	11.7	23.88	25.97	8.77
500 °C	Aromatics	1.80	1.955	6.93	25.44	27.34	7.50
510 °C	Aromatics	1.97	2.056	6.54	26.56	28.73	8.17

Figures (26) and (27) show that predicted temperature profiles along bed length at temperatures 480 and 490 °C for tri and bi-metal catalyst. It can be seen that from these figures the temperature profile decreases along the catalyst bed length (for all temperature ranges). This result of heavy naphtha catalytic reforming process trend agrees with the published results. Because reforming process reactions are, overall, endothermic many researches indicate that the temperature decreases along the catalyst bed, therefore to maintain reaction temperature at operatable levels commercial catalytic reformers are designed with multiple reactors with heaters between the reactors [16, and 21].

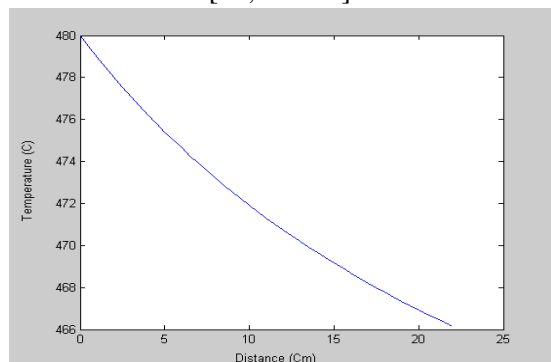


Figure (26) Temperature profile simulation at 480 °C

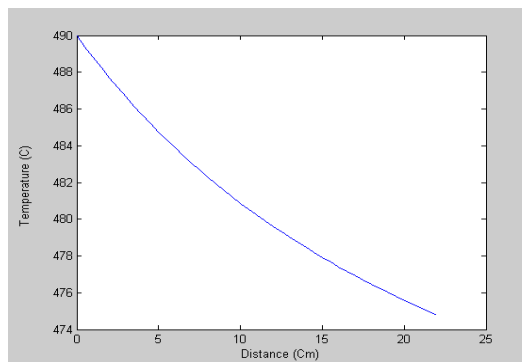


Figure (27) Temperature profile simulation at 490 °C

and (1hr-1)of for tri-metal catalyst.

and (1hr-1)of for bi-metal catalyst.

## 6. Conclusions

The selectivity of catalysts for Iraqi heavy naphtha reactants toward aromatization reactions for light aromatics (A6, and A7) increases, by improving the catalysts through addition of iridium (Ir) and tin (Sn) as bi-metal and tri-metal catalysts to Al-Dura refinery catalysts used in reforming units. Paraffins and Naphthenes conversion for heavy naphtha increases with increasing of reaction temperature Tri-metal catalyst the conversion % for Paraffins increasing from (11.50 % - 22.58 %), Naphthenes (56 % - 67 %) for), whilst the bi-metal catalyst conversion% for Paraffins increasing from (8.57 % - 16.7 %) and for Naphthenes (50 % - 63.15 %). On the other hand when increasing of weight hour space velocity conversion % decreases.

Aromatics products yield increases with an increase in reaction temperature. Tri-metal catalyst increasing from (25.8 % - 32.12 %), and for bi-metal catalyst increasing from (24.51% - 29.41%) while aromatics products decreasing when increasing of weight hour space velocity. Simulation and progressing model agreement with the results of experimental work according to the suggested scheme for heavy naphtha catalytic reforming of network.reactions, the deviation results when comparison of experimental and model results equal to 19.5%.

## NOMENCLATURE

Symbol	Definition	Units	Symbol	Definition	Units
A	Aromatics	(-)	$K_{e2}$	Reaction equil. constant	(-)
A <sub>0</sub>	Pre-exponential factor	(-)	LHSV	Liquid hour space velocity	hr <sup>-1</sup>
A <sub>i</sub>	Aromatics(6,7,8,9) carbon atom	(-)	Mwt	Molecular weight	g/gmole
C <sub>N</sub>	Naphthenes concentration	mole/cm <sup>3</sup>	N <sub>i</sub>	Naphthene (5,6,7,8,9) C-atom	(-)
C <sub>n0</sub>	Initial concentration of species n	mole/cm <sup>3</sup>	n-P <sub>i</sub>	Paraffine(5,6,7,8,9,10)C- atom	(-)
C <sub>n</sub>	Concentration of species n	mole/cm <sup>3</sup>	P	Paraffin	(-)
C <sub>p</sub>	Specific heat	J/mole.°C	P <sub>2</sub>	Total pressure	atm
E <sub>a</sub>	Activation energy	kJ/mole	R	Gas constant	J/mole.K
F <sub>n0</sub>	Initial molar flow rate of species n	mole/hr	r <sub>i</sub>	Reaction rate of species i	mole/gcat. hr
F <sub>n</sub>	Molar flow rate of species n	mole/hr	T	Reaction temperature	°C
f	Weight flow rate	g / hr	T <sup>*</sup>	Initial temperature	°C
G	Gases	(-)	V	Volume	cm <sup>3</sup>
GC	Gas chromatography	(-)	V <sub>g</sub>	Volume of gas adsorbed	cm <sup>3</sup>
H <sub>2</sub>	Hydrogen	(-)	V <sub>c</sub>	Volume of catalyst	cm <sup>3</sup>
ΔH <sub>r</sub>	Heat of i th reaction	J/ mole	W	Weight of catalyst	kg
H <sub>2</sub> /H.C	Hydrogen to hydrocarbon mole ratio	(-)	WHSV	Weight hour space velocity	hr <sup>-1</sup>
iso-P	Iso-paraffins	(-)	Y <sub>i</sub>	Molar composition of species i (A, N, and P)	(-)
k	Reaction rate constant	hr <sup>-1</sup>	zt	Length of reactor	cm
r <sub>2</sub>	React. rate for naphthene's dehydrogenation reaction	mole/gcat. hr	Δz	Integration step for the reactor length	(-)
ρ <sub>c</sub>	Density	Kg/m <sup>3</sup>	ε	Porosity of catalyst bed	(-) cm <sup>3</sup> /cm <sup>3</sup>

## References

- [1] Ali Al-Shathr, Zaidoon M. Shakor, Hasan Sh. Majdi, Adnan A. AbdulRazak, and Talib M. Albayati , " Comparison between Artificial Neural Network and Rigorous Mathematical Model in Simulation of Industrial Heavy Naphtha Reforming Process", *Catalysts*, 11, 1034. <https://doi.org/10.3390/catal11091034>, 2021.
- [2] Mbinzi K. D. Ngwanzaa, Diakanua B. Nkazi b, Hugues S. Ngwanzac Hembe E. Mukayad. " Review of Catalytic Processes Design and Modeling:Fluid Catalytic Cracking Unit and Catalytic Reforming Unit ". *International Journal of Research & Review (www.ijrrjournal.com)*., Vol.5; Issue: 11; November 2018 .
- [3] Pishnamazi M, Taghvaie Nakhjiri A, Rezakazemi M, Marjani A, Shirazian S Mechanistic modeling and numerical simulation of axial flow catalytic reactor for naphtha reforming unit. *PLoS ONE* 15(11): e0242343. <https://doi.org/10.1371/journal.pone.0242343>, 2020.
- [4] Aminu Zakari Yusuf 1,2, B.O. Aderemi 3, Raj Patel 1 and Iqbal M. Mujtaba," Study of Industrial Naphtha Catalytic Reforming Reactions via Modelling and Simulation", *Processes*, 7, 192; doi:10.3390/pr7040192, [www.mdpi.com/journal/processes](http://www.mdpi.com/journal/processes), 2019.
- [5] Chang Lin, Zitu Yang, Huihua Pan, Jia Cui, Zhi Lv, Xianglin Liu, Pengfei Tian, Zhikai Xiao, Ping Li, Jing Xu, Yi-Fan Han," Ce-introduced effects on modification of acidity and Pt electronic states on Pt-Sn/ $\gamma$ -Al<sub>2</sub>O<sub>3</sub> catalysts for catalytic reforming ", *Applied Catalysis A: General Volume* 617, 5 May 2021, 118116.
- [6] Nada S. Ahmedzeki, Ban A. Al-TabbakhBan, Maher B. Antwan Selahattin Yilmaz, "Heavy naphtha upgrading by catalytic reforming over novel bi-functional zeolite catalyst ", *Reaction Kinetics, Mechanisms and Catalysis* 125(2), July 2018.
- [7] Askari A., Karimi H., Rahimi M.R., Ghanbari M., "Simulation and Modeling of Catalytic Reforming Process", *J. Petroleum and Coal*, vol 54, No (1), p 76-84, 2012.
- [8] Elizalde, I.; Ancheyta, J. Dynamic modeling and simulation of a naphtha catalytic reforming reactor. *Appl. Math. Model.* 39, 764–775, 2015.
- [9] Dong, X.J.; He, Y.J.; Shen, J.N.; Ma, Z.F. Multi-zone parallel-series plug flow reactor model with catalyst deactivation effect for continuous catalytic reforming process. *Chem. Eng. Sci.*, 175, 306–319, 2018.
- [10] Xiaoyang Yi, Peng Zhang and Changlu Hu," Detailed description of the mathematical modeling of the catalytic naphtha reforming process dynamics", *IOP Conf. Series: Materials Science and Engineering* 729 012095 doi:10.1088/1757-899X/729/1/012095, (2020).
- [11] Fogler S.C.,” *Element of Chem. React. Eng.*”, 2<sup>nd</sup> Edi., Prentice-Hall of India Private Limit., (1997).

- [12] Aguilar R.E., Ancheyta J.J., " New Process Model Proves Accurate in Tests on Catalytic Reformer", Oil Gas J., vol. 25, p 80-83, (1994).
- [13] Gates B.C., Katzer J.R., Schuult G.C.A., " Chemistry of Catalytic Processes", McGraw-Hill book Co. New York, p 184, (1979).
- [14] Villafertre E., Jorge A.J., " Kinetic and Reactor Modeling of Naphtha Reforming Process", J. Petroleum and Coal, vol. 44, 1-2, p 63-66, (2002).
- [15] Lu H., " Manual of Petrochem. Indu. Fund. Data", Chem. Indu. Press, Beijing, China, (1982).
- [16] Rasaei, Yasaman; Towfighi Darian, Jafar, " Experimental Investigation and Kinetic Modeling of Naphtha Catalytic7 Reforming Using Pt-Re/Al<sub>2</sub>O<sub>3</sub> Catalyst ", Iran. J. Chem. Chem. Eng. Vol. 40, No. 1, 2021
- [18] Vanina A.M., Javier M.G., Carlos R.V., Juan C.Y., José M.P., Carlos C.Y., " Role of Sn in Pt-Re-Sn/AL<sub>2</sub>O<sub>3</sub>-Cl Catalysts for Naphtha Reforming ", J. Catal Today, vol 107-108, p 643-650,(2005).
- [19] Bednarova L., Lyman C.E., Rytter E., Holmen A., J. Catal, vol. 211, p 335, (2002).
- [20] Mohammed A.A., Hussein K.H., " Catalytic Aromatization of Naphtha Using Different Catalysts", Iraq. J. Chem. and Petr. Eng, vol. 5, (Dec), p 13, (2004).
- [21] Elizalde, I.; Ancheyta, J. Dynamic modelling and simulation of a naphtha catalytic reforming reactor. Appl. Math. Model., 39, 764–775, 2015.
- [22] Ramzy.S. H; Shakoor, Z.M.; Jawad, A.A. Prediction of Reaction Kinetic of Al-Doura Heavy Naphtha Reforming Process Using Genetic Algorithm. Al-Khwarizmi Eng. J., 10, 47–61, 2014.